


Emergent Fermi Surface in a Triangular-Lattice SU(4) Quantum AntiferromagnetAnna Keselman,¹ Bela Bauer,² Cenke Xu,³ and Chao-Ming Jian²¹*Kavli Institute for Theoretical Physics, University of California, Santa Barbara, California 93106-4030, USA*²*Microsoft Station Q, Santa Barbara, California 93106-6105, USA*³*Department of Physics, University of California, Santa Barbara, California 93106, USA* (Received 16 December 2019; revised 18 June 2020; accepted 10 August 2020; published 9 September 2020)

Motivated by multiple possible physical realizations, we study the SU(4) quantum antiferromagnet with a fundamental representation on each site of the triangular lattice. We provide evidence for a gapless liquid ground state of this system with an emergent Fermi surface of fractionalized fermionic partons coupled with a U(1) gauge field. Our conclusions are based on numerical simulations using the density matrix renormalization group method, which we support with a field theory analysis.

DOI: [10.1103/PhysRevLett.125.117202](https://doi.org/10.1103/PhysRevLett.125.117202)

Realizations of quantum spin liquids—quantum phases of spins whose ground state is not described by local ordering patterns but instead characterized by exotic quantum entanglement—have been highly sought after since such a phase was first hypothesized [1]. Within the broad family of spin liquids, a particularly elusive category is gapless spin liquids that exhibit gapless excitations on an extended region in the momentum space, akin to the Fermi surface in ordinary metals. These states of matter thus bear a resemblance to metals when (thermal) transport or thermodynamic properties, such as magnetic susceptibility or specific heat, are considered, even though charge degrees of freedom are frozen in the system. The known realizations of such gapless phases in systems of SU(2) spins usually require complicated Hamiltonians beyond the Heisenberg interaction, such as ring exchange terms [6–14], staggered chiral three-spin interactions [15,16], or antiferromagnetic Kitaev interactions in an external field [17–19].

Here, we report strong evidence for a gapless liquid with an emergent Fermi surface of fractionalized partons in the nearest-neighbor SU(4) Heisenberg quantum antiferromagnet on the triangular lattice with a fundamental representation on each site. While SU(N) antiferromagnets were suspected to harbor exotic phases already in the early days of the field [20–26] and recent work has demonstrated the presence of a Dirac spin liquid in the same model on the honeycomb lattice [27], our motivation for studying this model stems primarily from the availability of several possible experimental realizations. In transition metal compounds, spin and orbital degrees of freedom may be described by an effective SU(4) quantum magnet [28–31]. Cold atomic gases formed by atoms with large hyperfine spin component can form effective SU(N) quantum antiferromagnet [32], and spin-3/2 atoms can naturally form Sp(4) or SU(4) quantum antiferromagnet [33–35] when only the s -wave scattering between the atoms is considered. Most recently, it was also proposed that some of the 2D

systems with moiré superlattices may be described by an approximate SU(4) quantum antiferromagnet [36–40] at commensurate fillings where correlated insulators were observed recently [41–43].

In the following, we will first introduce a parton mean-field construction for a candidate liquid state for the model. We then carefully examine the properties of this state when placed on quasi-one-dimensional cylinder geometries, including the effects of symmetry-allowed perturbations specific to these geometries. These will also be the target of unbiased numerical simulations using the density-matrix renormalization group (DMRG) method [44,45]. We find our numerical results to be in agreement with predictions from the field theory that describes the proposed liquid state. For two cases of even circumference, we find gapped states with ordering patterns which are consistent with the one-dimensional field theory that contains relevant symmetry-allowed perturbations deviating from a gapless fixed point; while in a case with odd circumference, where there are no relevant translation-symmetric operators, we find a gapless state whose structure factor exhibits sharp features consistent with the field theory. We thus conclude that our proposed theory describes the system accurately in quasi-one-dimensional geometries and thus likely also in the two-dimensional limit.

Model.—We study the Kugel-Khomskii model [46] on the two-dimensional triangular lattice at the SU(4) symmetric point,

$$H = J \sum_{\langle ij \rangle} \left(2\mathbf{S}_i \cdot \mathbf{S}_j + \frac{1}{2} \right) \left(2\mathbf{V}_i \cdot \mathbf{V}_j + \frac{1}{2} \right), \quad (1)$$

where $J > 0$ is an antiferromagnetic coupling and \mathbf{S}_i (\mathbf{V}_i) denote the $S = 1/2$ spin (orbital) degrees of freedom at site i . We denote the three Pauli matrices that act on the twofold spin (orbital) indices as σ^a (τ^a), such that $S^a = \sigma^a/2$

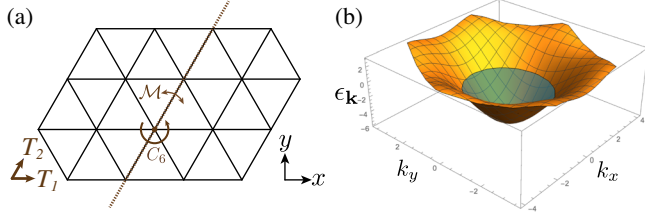


FIG. 1. (a) T_1 and T_2 denote the translation symmetries along the two basis vectors of the 2D triangular lattice. \mathcal{M} denotes the mirror symmetry with the T_2 direction as the mirror plane and C_6 denotes the sixfold crystal rotation symmetry. (b) The parton mean-field band structure (orange) and the Fermi level corresponding to filling $\nu = 1/4$ (blue).

($V^a = \tau^a/2$) with $a = x, y, z$. We can view the degrees of freedom on each site as a pseudospin in the fundamental representation of $SU(4)$, with the 15 operators $\{\sigma^a, \tau^b, \sigma^a \tau^b\}_{a,b=x,y,z}$ being the 15 generators of $SU(4)$. The Hamiltonian Eq. (1) can be interpreted as an $SU(4)$ antiferromagnetic Heisenberg model.

The Hamiltonian Eq. (1) is invariant under the global $SU(4)$ pseudospin rotation symmetry, as well as the spatial symmetries of the triangular lattice including the translation symmetries $T_{1,2}$, the mirror symmetry \mathcal{M} , and the sixfold rotation symmetry C_6 , as shown in Fig. 1(a). In addition, as a spin-orbital system, the model naturally admits a time-reversal symmetry [47].

Fermionic parton mean-field ansatz.—We now construct a candidate for the ground state of the model in Eq. (1). We start by introducing a four-component fermionic parton on each site, and use $f_{i,m=1,\dots,4}$ ($f_{i,m}^\dagger$) to denote the corresponding annihilation (creation) operators. The four components of the fermionic parton can also be labeled by the twofold spin indices and twofold orbital indices. They transform into each other under the global $SU(4)$ pseudospin rotation. The $SU(4)$ pseudospin operators (on the site i) can be represented in terms of the fermionic parton as

$$\begin{aligned} S_i^a &= \frac{1}{2} f_i^\dagger \sigma^a f_i, & V_i^b &= \frac{1}{2} f_i^\dagger \tau^b f_i, \\ (S^a V^b)_i &= \frac{1}{4} f_i^\dagger \sigma^a \tau^b f_i. \end{aligned} \quad (2)$$

The physical Hilbert space of $SU(4)$ pseudospins is obtained from the Hilbert space of the fermionic partons by imposing the constraint $n_i = \sum_{m=1}^4 f_{i,m}^\dagger f_{i,m} = 1$ on each site i .

In terms of the fermionic partons, the Hamiltonian in Eq. (1) consists of four-fermion interaction terms. At the mean-field level, different decouplings of these interactions can be considered. We examine the simplest decoupling which preserves the full $SU(4)$ pseudospin rotation symmetry and the space-group symmetries of the triangular lattice, by introducing a mean field $\chi_{ij} = \langle \sum_{m=1}^4 f_{i,m}^\dagger f_{j,m} \rangle$ on every bond. Assuming χ_{ij} takes the same value χ on

each bond (which is enforced by the space-group symmetry), we arrive at the mean-field Hamiltonian,

$$H_{\text{mf}} = -t \sum_{\langle ij \rangle} \sum_{m=1}^4 f_{i,m}^\dagger f_{j,m} + \text{H.c.}, \quad (3)$$

which contains only uniform nearest-neighbor parton hoppings and where $t \propto J\chi$. We will take $t > 0$ and use this Hamiltonian as an ansatz, i.e., not perform any self-consistent analysis.

This mean-field ansatz yields a single fourfold-degenerate parton band. At the mean-field level, the single-occupancy constraint $n_i = 1$ requires the partons have filling factor $\nu = 1/4$ and, hence, results in a parton Fermi surface as shown in Fig. 1(b). Beyond mean field, the constraint above can be implemented by a dynamical $U(1)$ gauge field coupled to the fermionic partons.

Finite circumference cylinders.—Our numerical simulations will be performed predominantly for cylinder geometries that are constructed by compactifying the T_2 direction and imposing periodic boundary conditions on the $SU(4)$ pseudospin variables [see Fig. 2(a)]. The circumference of the cylinder is denoted as W and the length as L . The quasi-1D system with finite W (and infinite L) maintains the space-group symmetry $T_{1,2}$ and \mathcal{M} but breaks the C_6 symmetry to a twofold crystal rotation symmetry C_2 .

Placing the mean-field Hamiltonian (3) on this geometry requires additionally specifying the boundary condition for the partons in the T_2 direction. The only choices that preserve the product of mirror and rotation symmetries $\mathcal{M}C_2$ are periodic and antiperiodic boundary conditions. These can also be interpreted as placing a $U(1)$ gauge flux

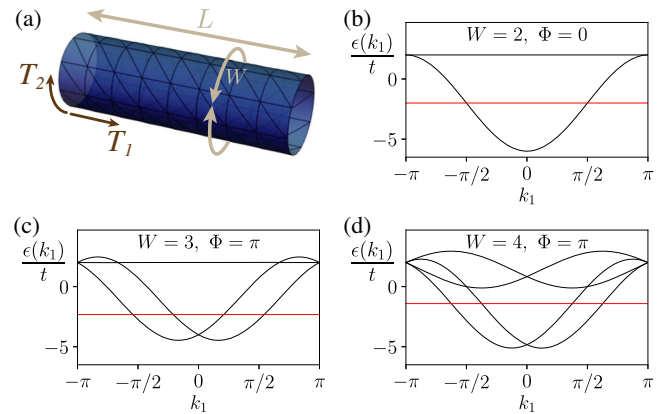


FIG. 2. (a) Compactification of the 2D lattice along the T_2 direction, resulting in a cylinder geometry. (b)–(d) The parton mean-field band structure on the compactified, quasi-1D geometry, when the number of unit cells along T_2 is $W = 2, 3, 4$, respectively. Boundary conditions along the T_2 direction considered here are periodic ($\Phi = 0$) for $W = 2$ and antiperiodic ($\Phi = \pi$) for $W = 3, 4$.

$\Phi = 0$ and $\Phi = \pi$, respectively, through the cylinder. In general, there is not a simple reasoning which value of Φ is more favorable for a certain geometry. We can view it as a discrete parameter (our only parameter) when comparing the parton ansatz and the results of the DMRG study.

For finite W , the two-dimensional parton band structure reduces to W (fourfold-degenerate) one-dimensional bands, distinguished by their crystal momentum k_2 along the T_2 direction, and parametrized by the crystal momentum k_1 along the T_1 direction. The parton Fermi level is still determined by the parton filling constraint $\nu = 1/4$. In general, the number of (partially) occupied one-dimensional parton bands depends on both W and Φ . In the following, we will focus on the $\Phi = 0$ scenario for $W = 2$ and $\Phi = \pi$ for $W = 3, 4$, as we find that these choices are most consistent with the DMRG results. The corresponding one-dimensional band structures are shown in Figs. 2(b)–2(d). A more comprehensive comparison with different choices of Φ for $W = 2, 3, 4$ is given in the Supplemental Material [47]. The Fermi momenta for each W can be calculated directly from the mean-field Hamiltonian Eq. (3). For $W = 2$ with $\Phi = 0$, the single partially occupied band has $k_2 = 0$ and the k_1 values of the Fermi momenta are $\pm\pi/2$. For $W = 3, 4$ with $\Phi = \pi$, the two bands that are (partially) occupied by the partons have crystal momenta $k_2 = \pm\pi/W$ and the k_1 values of the four Fermi momenta are $\pm\pi/(2W) \pm \pi W/8$. In fact, in all the cases we consider, these Fermi momenta are also completely fixed by the symmetries [47].

For each W , by linearizing the parton bands around each Fermi point, we obtain a continuum Lagrangian of low-energy partons:

$$\mathcal{L}_W^{(0)} = \sum_{r,n,m} [\psi_{r,n,m}^\dagger (i\partial_0 + v_r i\partial_1) \psi_{r,n,m}]. \quad (4)$$

Here $\mu = 0, 1$ label the temporal and spatial components. The fermionic fields $\psi_{r,n,m}$ describe the low-energy partons near the Fermi points, where m is the SU(4) pseudospin index, n is the band index, and $r = R$ (L) stands for right (left) movers with a velocity $v_{r,n} = \pm v_n$, respectively. In all the scenarios we consider, the Fermi points in a given geometry are all related by symmetries (\mathcal{T} , \mathcal{M} , and C_2), so are the respective velocities. Thus, we find that the Lagrangian in Eq. (4) describes SU(4)-invariant massless Dirac fermions for $W = 2$, whereas for $W = 3, 4$ it describes massless Dirac fermions with an enhanced SU(8) symmetry.

Going beyond the mean-field level, the parton filling constraint, $n_i = 1$, leads to the coupling of the low-energy fermions in Eq. (4) to a dynamical U(1) gauge field a_μ , via the substitution $i\partial_\mu \rightarrow i\partial_\mu - a_\mu$. Thus, the low-energy theory for $W = 2$ ($W = 3, 4$) is given by the $N_f = 4$ ($N_f = 8$) QED₂, or equivalently the 1 + 1D SU(4)₁ [SU(8)₁] conformal field theory (CFT), whose energy

spectrum is gapless. The Dirac mass terms are forbidden in all of these cases due to the translation symmetry T_1 .

We next consider symmetry-allowed relevant perturbations to these gapless theories. More specifically, we will focus on possible umklapp scatterings for each W . Although these perturbations are not expected to appear in the 2D limit, we will see that they can change the low-energy physics dramatically for the cases with finite circumferences we study numerically.

For $W = 2$, the distance between the two Fermi points is π , and thus allows for the following symmetry-preserving umklapp interaction,

$$\mathcal{L}_{W=2,\Phi=0}^{\text{int}} = \left(\sum_{m=1}^4 \psi_{L,m}^\dagger \psi_{R,m} \right)^2 + \text{H.c.}, \quad (5)$$

where we suppressed the band index in the fields $\psi_{L,m}^\dagger$ and $\psi_{R,m}$ because there is only one (partially) occupied band. Using the Fierz identity, this interaction can be written as a backscattering between left-moving and right-moving primary fields in the SU(4)₁ CFT, both carrying the six-dimensional representation of SU(4) [47]. In the SU(4)₁ CFT, each of such primary fields has scaling dimension 1/2. Therefore, the umklapp interaction has scaling dimension 1 and, hence, is a relevant perturbation. It can lead to a phase with a finite vacuum expectation value $\langle \sum_{m=1}^4 \psi_{L,m}^\dagger \psi_{R,m} \rangle$ that gaps out all low-energy degrees of freedom and spontaneously breaks the T_1 -translation symmetry by doubling the unit cell in the T_1 direction. Other symmetries stay intact in this gapped phase. In fact, for $W = 2$, doubling of the unit cell along the T_1 direction in a gapped phase is expected due to the 1D Lieb-Schultz-Mattis constraint for SU(4) spin chains [48].

For $W = 3$, due to the (relative) positions of the Fermi points, the symmetry-allowed umklapp terms are of high orders (i.e., at least 16) in terms of the low-energy fermion fields. Therefore, their effect can be neglected, and the SU(8)₁ CFT (or equivalently the $N_f = 8$ QED₂) remains a good description of the system. With $W = 3$, each unit cell in the T_1 direction has three SU(4) pseudospins. In the absence of T_1 symmetry breaking, the system has to be gapless based on the SU(4) Lieb-Schultz-Mattis constraint [48].

For $W = 4$, the distance between the two Fermi points within each band is π , and thus allows for the following symmetry-preserving umklapp interactions,

$$\left(\sum_m \psi_{L,n,m}^\dagger \psi_{R,n,m} \right) \left(\sum_m \psi_{L,n',m}^\dagger \psi_{R,n',m} \right) + \text{H.c.}, \quad (6)$$

where $n, n' = 1, 2$ label the two 1D parton bands that are (partially) occupied. These interactions can all be written as the backscattering between left-moving and right-moving primary fields in the SU(8)₁ CFT which both carry the 28-dimensional representation of SU(8) [47]. In the SU(8)₁

CFT, each of such primary fields has a scaling dimension $3/4$. Therefore, each of these umklapp interactions has a scaling dimension $3/2$ and again is a relevant perturbation. These perturbations can lead to a phase with nonzero $\langle \sum_{m=1}^4 \psi_{L,n,m}^\dagger \psi_{R,n,m} \rangle$ (for both $n = 1, 2$) that gap out the system while breaking the T_1 -translation symmetry by doubling the unit cell. Other symmetries remain intact in this gapped phase. Interestingly, for $W = 4$, each unit cell along the T_1 has four SU(4) pseudospins. Thus, in this case, the SU(4) Lieb-Schultz-Mattis constraint does not require a gapped phase to break the T_1 -translation symmetry. As we will demonstrate, the DMRG with $W = 4$ also shows a doubling of the unit cell, which is consistent with our field theory analysis.

Numerical study.—We perform DMRG simulations using the ITensor library [49]; to accelerate the simulations, we explicitly conserve three U(1) quantum numbers corresponding to total S^z , V^z , and $S^z V^z$. A key observable is the pseudospin gap Δ , which we obtain as the energy difference between the ground states in the sectors with $(S^z, V^z, S^z V^z) = (0, 0, 0)$ [which contains the SU(4) singlet] and $(S^z, V^z, S^z V^z) = (1, 0, -1/2)$. For each cylinder circumference W , we obtain the gap Δ for cylinders of varying length and then perform an extrapolation to the thermodynamic limit.

The gap obtained for $W = 2, 4$ is shown in Figs. 3(a) and 3(c). In both cases, we find that the gap remains finite in the limit of $L \rightarrow \infty$, consistent with the expectation of a gapped phase due to the umklapp scattering. Translation-symmetry breaking can be observed directly in the bond expectation values $\langle \sum_\alpha S_i^\alpha \cdot S_j^\alpha \rangle$, where S^α are the 15 SU(4) pseudospin

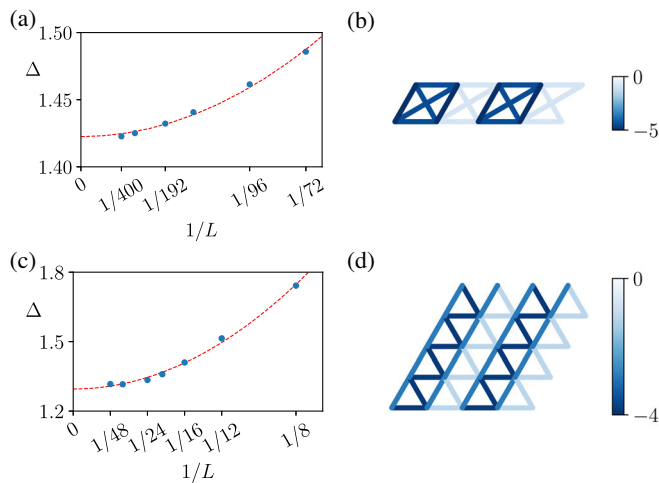


FIG. 3. (a),(c) Finite-size scaling of the pseudospin gap for cylinders of width $W = 2, 4$ obtained using a bond dimension of up to $M = 4000$, resulting in truncation errors of $\epsilon_{\text{tr}} \simeq 10^{-5}$ ($\epsilon_{\text{tr}} \simeq 10^{-9}$) for $W = 4$ ($W = 2$). Red dashed line is a fit to $\Delta_0 + a/L^2$ yielding $\Delta_0 = 1.42$ for $W = 2$ and $\Delta_0 = 1.29$ for $W = 4$. (b),(d) Bond expectation values for the middle four rungs in a cylinder of length $L = 24$ and width $W = 2, 4$, respectively.

operators $\{\sigma^a, \tau^b, \sigma^a \tau^b\}_{a,b=x,y,z}$ and i, j are a pair of nearest-neighbor sites. The pattern of bond expectation values is shown for the middle four rungs in a cylinder of length $L = 24$ and circumference $W = 2, 4$ in Figs. 3(b) and 3(d). Unit cell doubling along T_1 can be clearly seen in both cases. We emphasize that for $W = 4$, no translation-symmetry breaking along the circumference of the cylinder (i.e., along T_2) is observed [47], indicating that the state does not originate from plaquette coverings of the lattice as proposed in Refs. [26,50]. We also consider an alternative compactification on the cylinder with circumference $W = 4$ [47] that is chosen to be compatible with the 12-site valence-bond-solid-ordered (VBS-ordered) state that was proposed as candidate ground state in Ref. [26]. In this geometry, we find further evidence for the validity of the parton construction, and no indications for the formation of a 12-site VBS.

The finite-size behavior of the gap for $W = 3$ is shown in Fig. 4(a). Although the results for the gap are not fully conclusive, they are consistent with either a vanishing or a very small gap. Here, a bond dimension of up to $M = 8000$ was used, resulting in a truncation error of $\epsilon_{\text{tr}} \simeq 5 \times 10^{-5}$ for the ground state. Since the truncation errors in the $S^z = 1$ sector were slightly higher, to obtain a more accurate value for the gap we performed an extrapolation of the energy with truncation error in each sector before subtracting the two [47].

To understand the nature of the state in this case, we consider the static SU(4)-pseudospin structure factor,

$$\mathcal{F}(\vec{k}) = \sum_i e^{i\vec{k} \cdot (\vec{r}_i - \vec{r}_{i_0})} \sum_\alpha \langle S_i^\alpha \cdot S_{i_0}^\alpha \rangle, \quad (7)$$

where \vec{r}_i, \vec{r}_{i_0} denote the positions of the sites i, i_0 . For a gapless state with a parton Fermi surface, the structure

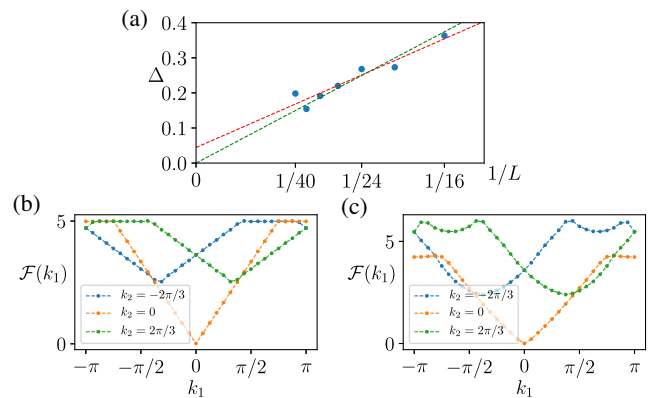


FIG. 4. (a) Finite-size scaling of the pseudospin gap for cylinders of circumference $W = 3$. Red dashed line is a linear fit, while the green dashed line is a fit to $\Delta = a/L$. (b),(c) Pseudospin structure factor obtained for a finite cylinder with $W = 3$ and length $L = 32$ with respect to a site in the middle of the system. (b) Noninteracting partons in the mean-field band structure with $\Phi = \pi$. (c) DMRG.

factor is expected to exhibit cusps at particular momenta corresponding to the “ $2k_F$ ” values of the Fermi sea. Figure 4(c) shows the structure factor calculated in the ground state of a length $L = 32$ cylinder using DMRG. Comparing it to the structure factor calculated for the mean-field ansatz with $\Phi = \pi$ using Wick’s theorem [Fig. 4(b)], we observe good qualitative agreement and in particular see that the cusps appear at the same momenta.

Finally, we note that starting from the mean-field ansatz, the coupling to the gauge field may be numerically implemented by a Gutzwiller projection, i.e., projecting the mean-field wave function to a single occupancy on each site. The correlations in the resulting state can be probed using Monte Carlo sampling of the projected wave function. Carrying out this projection, we find that although no symmetry breaking is observed for $W = 2, 4$, the power-law decay of the SU(4)-pseudospin correlation function $\sum_a \langle S_i^\alpha \cdot S_{i_0}^\alpha \rangle$ in both cases agrees with the CFT prediction. This suggests that the Gutzwiller projection does not capture the effect of the umklapp interactions which are particularly important to the cylinder geometries with $W = 2, 4$. For $W = 3$, we verify that the cusps in the structure factor remain at the same position in the momentum space as for the mean-field ansatz [47].

Discussion.—For the quasi-1D geometries with $W = 2, 3, 4$, the DMRG results agree well with the analysis based on the parton mean-field ansatz plus possible umklapp interactions. We emphasize that the symmetry-allowed umklapp interactions considered are all particular to certain geometries ($W = 2, 4$). They are not expected to appear in the 2D limit as there is no Fermi-surface nesting in the 2D band structure [shown in Fig. 1(b)] at filling $\nu = 1/4$. In the 2D limit, the U(1) gauge flux Φ also does not affect the parton Fermi surface. Therefore, we expect that the parton Fermi surface obtained from the mean-field ansatz Eq. (3) is stable in the 2D limit and provides a good candidate for the ground state of the SU(4)-symmetric Kugel-Khomskii model Eq. (1) on the triangular lattice.

In real materials with spin and orbital degrees of freedom, one can only expect an approximate SU(4)-pseudospin symmetry. A small SU(4)-symmetry-breaking perturbation is expected to split the fourfold degeneracy of the 2D parton Fermi surface. A more comprehensive investigation of the stability of the parton Fermi surface to SU(4)-symmetry-breaking perturbations and other non-Kugel-Khomskii-type interactions will be left for future studies.

This research is funded in part by the Gordon and Betty Moore Foundation through Grant No. GBMF8690 to UCSB to support the work of A. K. C. X. is supported by NSF Grant No. DMR-1920434, the David and Lucile Packard Foundation, and the Simons Foundation. Use was made of the computational facilities administered by the Center for Scientific Computing at the CNSI and MRL (an NSF MRSEC; DMR-1720256) and purchased through NSF CNS-1725797.

- [1] For recent reviews, see Refs. [2–5].
- [2] L. Savary and L. Balents, *Rep. Prog. Phys.* **80**, 016502 (2017).
- [3] Y. Zhou, K. Kanoda, and T.-K. Ng, *Rev. Mod. Phys.* **89**, 025003 (2017).
- [4] J. Knolle and R. Moessner, *Annu. Rev. Condens. Matter Phys.* **10**, 451 (2019).
- [5] C. Broholm, R. Cava, S. Kivelson, D. Nocera, M. Norman, and T. Senthil, [arXiv:1905.07040](https://arxiv.org/abs/1905.07040).
- [6] O. I. Motrunich and M. P. A. Fisher, *Phys. Rev. B* **75**, 235116 (2007).
- [7] D. N. Sheng, O. I. Motrunich, S. Trebst, E. Gull, and M. P. A. Fisher, *Phys. Rev. B* **78**, 054520 (2008).
- [8] D. N. Sheng, O. I. Motrunich, and M. P. A. Fisher, *Phys. Rev. B* **79**, 205112 (2009).
- [9] M. S. Block, R. V. Mishmash, R. K. Kaul, D. N. Sheng, O. I. Motrunich, and M. P. A. Fisher, *Phys. Rev. Lett.* **106**, 046402 (2011).
- [10] M. S. Block, D. N. Sheng, O. I. Motrunich, and M. P. A. Fisher, *Phys. Rev. Lett.* **106**, 157202 (2011).
- [11] R. V. Mishmash, M. S. Block, R. K. Kaul, D. N. Sheng, O. I. Motrunich, and M. P. A. Fisher, *Phys. Rev. B* **84**, 245127 (2011).
- [12] H.-C. Jiang, M. S. Block, R. V. Mishmash, J. R. Garrison, D. N. Sheng, O. I. Motrunich, and M. P. A. Fisher, *Nature (London)* **493**, 39 (2013).
- [13] W.-Y. He, X. Y. Xu, G. Chen, K. T. Law, and P. A. Lee, *Phys. Rev. Lett.* **121**, 046401 (2018).
- [14] R. V. Mishmash, J. R. Garrison, S. Bieri, and C. Xu, *Phys. Rev. Lett.* **111**, 157203 (2013).
- [15] R. G. Pereira and S. Bieri, *SciPost Phys.* **4**, 004 (2017).
- [16] B. Bauer, B. P. Keller, S. Trebst, and A. W. W. Ludwig, *Phys. Rev. B* **99**, 035155 (2019).
- [17] C. Hickey and S. Trebst, *Nat. Commun.* **10**, 530 (2019).
- [18] N. D. Patel and N. Trivedi, *Proc. Natl. Acad. Sci. U.S.A.* **116**, 12199 (2019).
- [19] Y.-F. Jiang, T. P. Devereaux, and H.-C. Jiang, *Phys. Rev. B* **100**, 165123 (2019).
- [20] N. Read and S. Sachdev, *Nucl. Phys.* **B316**, 609 (1989).
- [21] S. Sachdev, *Phys. Rev. B* **45**, 12377 (1992).
- [22] N. Read and S. Sachdev, *Phys. Rev. Lett.* **66**, 1773 (1991).
- [23] N. Read and S. Sachdev, *Phys. Rev. B* **42**, 4568 (1990).
- [24] N. Read and S. Sachdev, *Phys. Rev. Lett.* **62**, 1694 (1989).
- [25] D. S. Rokhsar, *Phys. Rev. B* **42**, 2526 (1990).
- [26] K. Penc, M. Mambrini, P. Fazekas, and F. Mila, *Phys. Rev. B* **68**, 012408 (2003).
- [27] P. Corboz, M. Lajkó, A. M. Läuchli, K. Penc, and F. Mila, *Phys. Rev. X* **2**, 041013 (2012).
- [28] S. K. Pati, R. R. P. Singh, and D. I. Khomskii, *Phys. Rev. Lett.* **81**, 5406 (1998).
- [29] Y. Q. Li, M. Ma, D. N. Shi, and F. C. Zhang, *Phys. Rev. Lett.* **81**, 3527 (1998).
- [30] Y. Tokura and N. Nagaosa, *Science* **288**, 462 (2000).
- [31] M. G. Yamada, M. Oshikawa, and G. Jackeli, *Phys. Rev. Lett.* **121**, 097201 (2018).
- [32] A. V. Gorshkov, M. Hermele, V. Gurarie, C. Xu, P. S. Julienne, J. Ye, P. Zoller, E. Demler, M. D. Lukin, and A. M. Rey, *Nat. Phys.* **6**, 289 (2010).

- [33] C. Wu, J.-p. Hu, and S.-c. Zhang, *Phys. Rev. Lett.* **91**, 186402 (2003).
- [34] C. Wu, *Phys. Rev. Lett.* **95**, 266404 (2005).
- [35] C. WU, *Mod. Phys. Lett.* **20B**, 1707 (2006).
- [36] C. Xu and L. Balents, *Phys. Rev. Lett.* **121**, 087001 (2018).
- [37] H. C. Po, L. Zou, A. Vishwanath, and T. Senthil, *Phys. Rev. X* **8**, 031089 (2018).
- [38] Y.-H. Zhang and T. Senthil, *Phys. Rev. B* **99**, 205150 (2019).
- [39] X.-C. Wu, A. Keselman, C.-M. Jian, K. A. Pawlak, and C. Xu, *Phys. Rev. B* **100**, 024421 (2019).
- [40] C. Schrade and L. Fu, *Phys. Rev. B* **100**, 035413 (2019).
- [41] G. Chen, L. Jiang, S. Wu, B. Lyu, H. Li, B. L. Chittari, K. Watanabe, T. Taniguchi, Z. Shi, J. Jung *et al.*, *Nat. Phys.* **15**, 237 (2019).
- [42] Y. Cao, V. Fatemi, A. Demir, S. Fang, S. L. Tomarken, J. Y. Luo, J. D. Sanchez-Yamagishi, K. Watanabe, T. Taniguchi, E. Kaxiras *et al.*, *Nature (London)* **556**, 80 (2018).
- [43] M. Yankowitz, S. Chen, H. Polshyn, Y. Zhang, K. Watanabe, T. Taniguchi, D. Graf, A. F. Young, and C. R. Dean, *Science* **363**, 1059 (2019).
- [44] S. R. White, *Phys. Rev. Lett.* **69**, 2863 (1992).
- [45] U. Schollwöck, *Rev. Mod. Phys.* **77**, 259 (2005).
- [46] K. I. Kugel and D. I. Khomski, *Sov. Phys. Usp.* **25**, 231 (1982).
- [47] See Supplemental Material at <http://link.aps.org/supplemental/10.1103/PhysRevLett.125.117202> for additional numerical results and field theory analysis.
- [48] I. Affleck and E. H. Lieb, *Lett. Math. Phys.* **12**, 57 (1986).
- [49] ITensor Library, <http://itensor.org/>.
- [50] M. van den Bossche, P. Azaria, P. Lecheminant, and F. Mila, *Phys. Rev. Lett.* **86**, 4124 (2001).